HAL
open science

Comparing atmospheric transport models for future regional inversions over Europe – Part 1: mapping the atmospheric CO2 signals

C. Geels, M. Gloor, Philippe Ciais, Philippe Bousquet, P. Peylin, A. T. Vermeulen, R. Dargaville, T. Aalto, J. Brandt, J. H. Christensen, et al.

To cite this version:

C. Geels, M. Gloor, Philippe Ciais, Philippe Bousquet, P. Peylin, et al.. Comparing atmospheric transport models for future regional inversions over Europe – Part 1: mapping the atmospheric CO2 signals. Atmospheric Chemistry and Physics, 2007, 7 (13), pp.3479. 10.5194/acp-7-3461-2007 . hal-00328509

HAL Id: hal-00328509

https://hal.science/hal-00328509v1

Submitted on 18 Jun 2008

HAL is a multi-disciplinary open access archive for the deposit and dissemination of scientific research documents, whether they are published or not. The documents may come from teaching and research institutions in France or abroad, or from public or private research centers.

L'archive ouverte pluridisciplinaire **HAL**, est destinée au dépôt et à la diffusion de documents scientifiques de niveau recherche, publiés ou non, émanant des établissements d'enseignement et de recherche français ou étrangers, des laboratoires publics ou privés.

Atmos. Chem. Phys., 7, 3461–3479, 2007
www.atmos-chem-phys.net/7/3461/2007/
© Author(s) 2007. This work is licensed
under a Creative Commons License.

Atmospheric Chemistry and Physics

Comparing atmospheric transport models for future regional inversions over Europe – Part 1: mapping the atmospheric CO_2 signals

C. Geels[1], M. Gloor[2], P. Ciais[3], P. Bousquet[3], P. Peylin[3], A. T. Vermeulen[4], R. Dargaville[3], T. Aalto[5], J. Brandt[1], J. H. Christensen[1], L. M. Frohn[1], L. Haszpra[6], U. Karstens[7], C. Rödenbeck[7], M. Ramonet[3], G. Carboni[8], and R. Santaguida[9]

[1]National Environmental Research Institute, University of Aarhus, 4000 Roskilde, Denmark
[2]University of Leeds, Leeds, UK
[3]Laboratoire des Sciences du Climat et de l-Environnement, UMR CEA-CNRS 1572, 91191 Gif-sur-Yvette, France
[4]Energieonderzoek Centrum Nederland (ECN), 1755 ZG Petten, The Netherlands
[5]Finnish Meteorological Institute Air Quality Research, Sahaajankatu 20E 00810 Helsinki, Finland
[6]Hungarian Meteorological Service P.O. Box 39, 1675 Budapest, Hungary
[7]Max-Planck-Institut für Biogeochemie, 07701 Jena, Germany
[8]CESI ApA, Via r. Rubattino 54, 20134 Milano, Italy
[9]Italian Air Force Meteorological Service, Via delle Ville, 40, 41029 Sestola (MO), Italy

Received: 25 January 2006 – Published in Atmos. Chem. Phys. Discuss.: 11 May 2006
Revised: 8 May 2007 – Accepted: 18 June 2007 – Published: 2 July 2007

Abstract. The CO_2 source and sink distribution across Europe can be estimated in principle through inverse methods by combining CO_2 observations and atmospheric transport models. Uncertainties of such estimates are mainly due to insufficient spatiotemporal coverage of CO_2 observations and biases of the models. In order to assess the biases related to the use of different models the CO_2 concentration field over Europe has been simulated with five different Eulerian atmospheric transport models as part of the EU-funded AEROCARB project, which has the main goal to estimate the carbon balance of Europe. In contrast to previous comparisons, here both global coarse-resolution and regional higher-resolution models are included. Continuous CO_2 observations from continental, coastal and mountain sites as well as flasks sampled on aircrafts are used to evaluate the models' ability to capture the spatiotemporal variability and distribution of lower troposphere CO_2 across Europe. $^{14}CO_2$ is used in addition to evaluate separately fossil fuel signal predictions. The simulated concentrations show a large range of variation, with up to ∼10 ppm higher surface concentrations over Western and Central Europe in the regional models with highest (mesoscale) spatial resolution.

The simulation – data comparison reveals that generally high-resolution models are more successful than coarse models in capturing the amplitude and phasing of the observed short-term variability. At high-altitude stations the magnitude of the differences between observations and models and in between models is less pronounced, but the timing of the diurnal cycle is not well captured by the models.

The data comparisons show also that the timing of the observed variability on hourly to daily time scales at low-altitude stations is generally well captured by all models. However, the amplitude of the variability tends to be underestimated. While daytime values are quite well predicted, nighttime values are generally underpredicted. This is a reflection of the different mixing regimes during day and night combined with different vertical resolution between models. In line with this finding, the agreement among models is increased when sampling in the afternoon hours only and when sampling the mixed portion of the PBL, which amounts to sampling at a few hundred meters above ground. The main recommendations resulting from the study for constraining land carbon sources and sinks using high-resolution concentration data and state-of-the art transport models through inverse methods are given in the following: 1) Low altitude stations are presently preferable in inverse studies. If high altitude stations are used then the model level that represents the specific sites should be applied, 2) at low altitude sites only the afternoon values of concentrations can be represented sufficiently well by current models and therefore afternoon values are more appropriate for constraining large-scale sources and sinks in combination with transport

Correspondence to: C. Geels
(cag@dmu.dk)

models, 3) even when using only afternoon values it is clear that data sampled several hundred meters above ground can be represented substantially more robustly in models than surface station records, which emphasize the use of tower data in inverse studies and finally 4) traditional large scale transport models seem not sufficient to resolve fine-scale features associated with fossil fuel emissions, as well as larger-scale features like the concentration distribution above the south-western Europe. It is therefore recommended to use higher resolution models for interpretation of continental data in future studies.

1 Introduction

Quantifying the distribution and variability of CO_2 fluxes between the Earth's surface and the atmosphere is essential to understand the present state and the future behavior of carbon pools and in turn radiative forcing of the earths surface associated with atmospheric CO_2. Detailed and accurate knowledge of sources and sinks for atmospheric CO_2 down to continental and regional scales is also required to monitor and assess the effectiveness of carbon sequestration and/or emission reduction policies, such as the Kyoto Protocol.

Atmospheric transport integrates over all CO_2 surface sources and sinks. Measurements of the atmospheric CO_2 concentration can therefore be used in principle to quantify surface fluxes over large scales by matching them with simulation predictions obtained with atmospheric transport models. This approach, known as inverse modelling, is still limited by sparse and uneven coverage of CO_2 monitoring stations. The current atmospheric global observation network consisted until recently of less than 100 stations and contained mainly discrete biweekly flask observations from remote oceanic or high altitude background locations. Consequently, the carbon balance of the continents remains very poorly constrained in inversions and its partitioning between land regions like Europe, North America and North Asia varies among different studies depending on the included stations (e.g. Fan et al., 1998; Rayner et al., 1999; Bousquet et al., 2000; Rödenbeck et al., 2003). Furthermore, when inversion results obtained with different atmospheric transport models are compared (Gurney et al., 2002, 2003), the spread in fluxes induced by transport model differences was found to be almost as large as the uncertainties arising from the lack of adequate observations, especially over the Northern Hemisphere continents.

Recently, many new stations on continents where CO_2 is measured continuously have been initiated, which can be used to constrain regional CO_2 fluxes on land (Law et al., 2002). Observation sites are chosen to be regionally representative and at the same time not too close to point-like sources like towns. Such continental-oriented network includes low-altitude surface stations (eg. Haszpra, 1999), hill and mountain sites (Aalto et al., 2002; Apadula et al., 2003; Schmidt et al., 2003), tall tower sampling of the lower part of the planetary boundary layer (Bakwin et al., 1998) and frequent aircraft profiling (Gerbig et al., 2003).

Unfortunately, the inverse modelling approach for estimating carbon sources/sinks on land, based on atmospheric concentration gradients, faces a dilemma. On the one hand, several studies indicate that continental data for constraining regional fluxes with sufficiently small uncertainty are needed (e.g. Gloor et al., 2000). On the other hand atmospheric CO_2 records from the vegetated continents are challenging to use in inverse calculations for three reasons: 1) signals on land during summer are highly variable because of the proximity to vegetation and the large fluxes associated with photosynthesis and respiration, 2) the complexity of near surface air flow particularly during night is not well resolved and hard to represent with models, and 3) the mismatch in scale between point-like sources associated particularly with anthropogenic fossil fuel emissions and model resolution. Thus, it is currently an open question how to best use continental data for source/sink estimation using transport models and inverse methods.

The resolution of atmospheric transport models traditionally used for inverse modeling of CO_2 is on the order of $2.5^\circ \times 2.5^\circ$ degrees longitude by latitude or coarser (like for example the models used in TransCom, see Gurney et al., 2003). Because of the heterogeneous nature of surface fluxes and transport over land this resolution is likely not sufficient to reduce uncertainties of land sources and sinks by employing the new continental data. However, recent studies indicate that higher resolution mesoscale models are able to capture the observed variability over the continents more realistically (Chevillard et al., 2002b; Kjellström et al., 2002; Geels, 2003; Geels et al., 2004) than traditional coarse grid models.

While there have been extensive intercomparisons of global coarse-resolution transport models on monthly and annual time-scales, (Law et al., 1996; Bousquet et al., 1996; Gurney et al., 2003) little attention has so far been paid to quantify model differences on synoptic to diurnal scales above the continents. Partly because coarse-resolution transport models can only poorly resolve the short-term variability, but also because data have not been available. Currently the TransCom group has a new experiment underway to look at synoptic and diurnal variations between models (Law et al., 2005).

Here we present a coarse-to-high resolution model intercomparison study that includes five models and recent continental CO_2 data from Western Europe measured during the course of the AEROCARB project (http://www.aerocarb.cnrs-gif.fr/) as a yard stick. The purpose of this paper is to estimate the variability of the results given by a representative range of different models due to the differences in the description of transport in each model. Thereby we can obtain a better understanding of how to use optimally the new

Table 1. Summary of grid set-up in the models. At European latitudes 0.5°×0.5° corresponds to approximately 40 km×50 km.

Grid setup	TM3	LMDZ	HANK	DEHM	REMO
Domain	Global	Global/zoom over Europe	NH/Europe	NH/Europe	Europe
Resolution	5°×3.75°	3.75°×2.5°/ 1.2°×0.8°	270 km×270 km/ 90 km×90 km	150 km×150 km/ 50 km×50 km	0.5°×0.5°
Size of domain [km^2]	Global	Global/ 0°−28° E×38°−57° N	17 550×17 550/ 12 100×12 100	14 400×14 400 4800×4800	8300×4400
Projection	Lat-long. grid	Lat-long. grid	Polar stereog.	Polar stereog.	Rot. sphere.
Vertical levels	19	19	27	20	20
Δz lowest level	81.8 m	150 m	25 m	80 m	60 m
Levels below 1500 m	6	4	10	9	6
Top of model	0 hPa	4 hPa	100 hPa	25 hPa	0 hPa
Vertical coor. system	Hybrid	Hybrid	Sigma	Sigma	Hybrid

Table 2. Summary of the forcing meteorology and physical parameterizations applied in the different models.

Meteorology and physics	TM3	LMDZ	HANK	DEHM	REMO
Initial/boundary data	NCEP	ECMWF	MM5/NCEP	MM5/ECMWF	REMO/ECMWF
Δt meteorology	6 h	6 h	1 h	3 h	At boundaries: 6 h, inside: 5 min
Meteorology	Off-line	Off-line	Off-line	Off-line	On-line
Vertical diffusion	1st order K-theory	1st order K-theory	In PBL: Holtslag and Boville (1993)	1st order K-theory	TKE- 2nd order

continental CO_2 data in combination with models in order to reduce the uncertainties of land sources and sinks estimates.

The models used in this study span a range of resolutions, numerical schemes for solving the advection equation, parameterizations of subgrid-scale processes and meteorological drivers. Identical carbon fluxes are used as surface input in all models. The input consist in yearly mean fossil fuel emissions, monthly mean air-sea exchange and hourly Net Ecosystem Exchange (NEE) fluxes with the land biosphere. By applying such a common set of surface fluxes, our model intercomparison offers the opportunity to identify the differences caused by differences in the simulated transport and mixing processes, related to model specific parameters like the resolution. The comparison covers July and December of 1998.

The paper starts with a short description of the five tracer transport models. Next a qualitative analysis of the model differences is carried out by comparing the simulated average CO_2 field over Europe. Thereafter the model results at both continental and oceanic background locations are evaluated against observed CO_2 records using quantitative statistical evaluation criteria. Finally the main findings as well as data selection and atmospheric sampling recommendations are discussed.

In a companion paper, the same five transport models are used for simulating ^{222}Rn, which due to the comparatively time-constant nature of its source field and its short lifetime is a useful tracer of vertical mixing and synoptic processes (Vermeulen et al., 2007[1]). Also, regional inversions using the same models for Europe are underway (Rivier et al., 2007[2]).

2 The set-up of the model comparison

2.1 The transport models

The five tracer transport models involved in this study cover a representative range of global and regional models used previously in various atmospheric trace gas studies. An overview of the model characteristics is given in Tables 1 and 2. In addition we briefly summarize below the main features of each model.

[1] Vermeulen, A. T., Ciais, P., Peylin, P., Gloor, M., Bousquet, P., Aalto, T., Brandt, J., Christensen, J. H., Dargaville, R., Geels, C., Heimann, M., Karstens, U., Levin, I., Ramonet, M., Rödenbeck, C., Pieterse, G., and Schmidt, M.: Comparing atmospheric transport models for regional inversions over Europe. Mapping the 222Rn Atmospheric Signals, Atmos. Chem. Phys. Discuss., in preparation, 2007.

[2] Rivier, L., Bousquet, P., Brandt, J., Ciais, P., Geels, C., Gloor, M., Heimann, M., Karstens, U., Peylin, P., Rayner, P., Rödenbeck, C., et al.: Comparing atmospheric transport models for regional inversions over Europe. Part 2: Estimation of the regional sources and sinks of CO_2 using both regional and global atmospheric models, Atmos. Chem. Phys. Discuss., in preparation, 2007.

TM3 is a global off-line atmospheric tracer transport model developed by Heimann (1996). Its spatial resolution is flexible and the model can be run with both coarser and finer spatial resolution than in the present study (see Table 1). TM3 is usually driven on a 6-hourly basis by re-analyzed meteorological fields from NCEP or ECMWF weather prediction centers, which have to be converted and interpolated in a preprocessing step.

LMDZ (version 3.3) is a global tracer transport version of the GCM model LMDZ (Hauglustaine et al., 2004). It is a grid point global primitive equation model, which can be used for simulations with different horizontal resolutions on the global scale. The grid resolution can vary in space, which permits horizontal regional zooming (see http://www.lmd.jussieu.fr/~lmdz/homepage.html). Here the results from LMDZ are from a global simulation with minimal resolution of $3.75^\circ \times 2.5^\circ$ longitude by latitude including a zoom over Europe of approximately $1.2^\circ \times 0.8^\circ$. Simulated large-scale horizontal advection is nudged to analyzed 6-hourly wind fields from ECMWF reanalyses. When compared with the models used in the Transcom 1 intercomparison experiment (Rayner and Law, 1995) (not shown), LMDZ tends to have strong large-scale horizontal as well as vertical mixing.

HANK is a nested regional transport-chemistry model recently developed by Hess and colleagues (2000) at NCAR. It is driven by meteorological fields simulated by the Fifth-Generation NCAR/Penn State Mesoscale Model (MM5) model system (Grell et al., 1995), which is nudged towards global reanalyses from National Center of Environmental Protection (NCEP). For additional information see http://acd.ucar.edu/models/HANK/. For the simulations performed for this paper a polar stereographic coordinate system with a coarse grid mesh centered at the North Pole and covering approximately two thirds of the Northern Hemisphere is used. Within this larger domain, a sub-domain with three times finer resolution and centered over Europe is embedded.

DEHM (Danish Eulerian Hemispheric Model) is a regional model that was initially developed to study long-range transport of sulphur into the Arctic (Christensen, 1997). The model has since then been further developed to include nesting capabilities (see Frohn et al., 2002) as well as different chemical species (Frohn, 2004; Christensen et al., 2004; Geels et al., 2004; Hansen et al., 2004). The MM5 model (Grell et al., 1995) is used as the meteorological driver for the model system, which in this setup is nudged towards reanalyses from the European Center for Medium Range Weather Forecast (ECMWF).

REMO (REgional MOdel) is a regional climate model based on the Europamodell (EM) of the German Weather Service (DWD) (Majewski, 1991). For almost 10 years, the Europamodell has been the operational regional weather forecast model of DWD. REMO has been extended to an on-line atmosphere-chemistry model (Langmann, 2000). In the present study REMO (version 5.0) includes the physical parametrization package of DWD and is operated in a diagnostic mode. The results of consecutive short-range forecasts (30 h) are used. REMO is started each day at 00:00 UTC from ECMWF operational analyses and a 30-h forecast is computed. To account for a spin-up time the first six hours of the forecast are neglected. By restarting the model every day from analyses, the model state is forced to stay close to the ECMWF analyzed weather situation.

Note that the models TM3 and HANK are driven by meteorological fields preprocessed by the National Center for Environmental Protection (NCEP) meteorology, while LMDZ, DEHM and REMO are driven by fields from the European Center for Medium Range Weather Forecast (ECMWF).

2.2 Prescribed surface fluxes

The net exchange of CO_2 used as input at the models lower boundary in the five models, consists of fossil fuel emissions, an air-sea CO_2 flux, and a land photosynthesis and respiration flux.

Fossil fuel CO_2 emissions are obtained from the EDGAR3.0 emission Database (Olivier et al., 1996). The data set is based on a combination of statistics on energy consumption, emission factors, and population density as well as information on the location of major point sources. The resulting global emissions have a $1^\circ \times 1^\circ$ spatial resolution and corresponds to the year 1990. Main features for Europe are as follows: emissions are high over Central to Western Europe with the highest emissions over the Benelux countries, Germany and Great Britain. Outside these regions emissions are much smaller.

Between 1990 and 1998, which is the year in focus in this study, emissions have decreased by approximately 30% over Eastern and Central Europe, but remained more or less constant over the Western part of Europe (Marland et al., 2003). A few studies of the ^{14}C isotopic composition of carbon indicates variations of fossil fuel emission on seasonal to diurnal timescales in Europe (Levin et al., 2003). The documentation is, nevertheless, sparse and those variations are neglected here, in absence of better resolved fossil CO_2 emission maps (e.g. Blasing et al., 2005).

Air-sea flux of CO_2 is prescribed according to the study of Takahashi and colleagues (1999), who combined a climatological distribution of sea-air pCO_2 differences and a wind-speed dependent gas exchange coefficient (Wanninkhof, 1992) parameterization to estimate monthly air-sea fluxes for the global ocean with a $4^\circ \times 5^\circ$ resolution for 1995. The northernmost part of the Atlantic Ocean acts as a net sink for atmospheric CO_2 throughout the year ($-0.46\,GtCy^{-1}$ north of 50° N in 1995). In this study we neglect interannual variability of air-sea fluxes. Also there is no consistency between the wind fields used to transport CO_2 in the models and those used to calculate the air-sea gas exchange.

Biosphere-atmosphere exchange of CO_2 (net ecosystem exchange (NEE)) is estimated by the Terrestrial Uptake and Release of Carbon (TURC) model (Ruimy et al., 1996; La-

font et al., 2002). TURC is a light-use efficiency model driven by radiation, temperature, and humidity fields from ECMWF and 10-days composite Normalized Difference Vegetation Index (NDVI) from the SPOT4-VEGETATION sensor launched in April 1998. For January 1998 the NDVI data from 1999 have been used. The resolution of the TURC version we used is $1^\circ \times 1^\circ$ and the calculated daily fluxes for 1998 are divided into gross primary production (GPP) and the components of Ecosystem Respiration (ER) consisting in maintenance, growth and heterotrophic respiration. In order to fully resolve the diurnal cycle, the daily fluxes have been redistributed among the 24 hours of the day using a simple scaling scheme following the main characteristic of the fluxes. Growth and heterotrophic respiration are assumed to be uniform throughout the day. GPP and maintenance respiration on the other hand are assigned a diurnal cycle following the incoming shortwave radiation and local air temperatures. In the TURC model, each vegetated grid point is forced to be carbon neutral on a yearly basis (i.e. annual mean NEE=GPP−ER=0). This assumption, commonly applied in studies of the seasonal variability in atmospheric CO_2 (Fung et al., 1987; Denning et al., 1996) is reasonable in our case since we focus the model evaluation on synoptic and diurnal timescales. Yet, it may bias the model-data comparison when looking at monthly concentration gradients among sites. Note that the TURC biospheric fluxes driven by ECMWF fields are naturally more consistent with the models using ECMWF winds (LMDZ, DEHM and REMO) than for the other models (TM3 and HANK).

The TURC predicted fluxes have been evaluated both by direct comparison with a few eddy covariance data in Europe (Aalto et al., 2004) and by indirect comparison against atmospheric CO_2 data after being transported in atmospheric models (Chevillard, 2001; Geels, 2003). These studies demonstrated that during summer the hourly TURC fluxes are generally reproducing quite well the observed diurnal cycle of NEE at most temperate forest eddy flux sites with regards to timing and amplitude at mid latitudes, while the diurnal NEE and hence the seasonal amplitude is underestimated at higher latitudes. Occasionally very high night-time respiration fluxes observed at some sites are also not properly captured by TURC.

To give an idea of the order of magnitude of the fluxes, we list here the strength of the total monthly flux for each source type within the REMO model domain ($36.52 \times 10^6\,km^2$). In July the biosphere is a net sink of -0.35 GtC ($-13.8\,gC\,m^{-2}$ land mo^{-1}), while a net source of 0.24 GtC ($9.08\,gC\,m^{-2}$ land mo^{-1}) during December. The ocean acts like a net sink of -0.05 GtC ($-3.47\,gC\,m^{-2}$ ocean mo^{-1}) and -0.03 GtC ($-2.10\,gC\,m^{-2}$ ocean mo^{-1}) in July and December, respectively. Total fossil fuel emission amount to 0.17 GtC each month ($6.76\,gC\,m^{-2}$ land).

The fluxes have been re-gridded from the original spatial resolution of $1^\circ \times 1^\circ$ or $4^\circ \times 5^\circ$ to the grid of each model. Thereby will the lower resolution models lose peak values e.g. in the fossil fuel emissions compared to the models with a higher resolution. This means that while the net flux across Europe may be the same, there will be larger spatial variability of fluxes in the higher resolution models (up to the resolution of the original surface fluxes).

2.2.1 Boundary and initial conditions

The lateral and upper boundary conditions vary from model to model. The REMO model has the smallest domain and sensitivity tests show that concentrations at its lateral boundaries transported inside the European domain can dominate the CO_2 signal, especially at higher altitude stations (Chevillard et al., 2002a,b). Here the global CO_2 fields used at REMO's boundaries are prescribed at a 3h interval from simulations with the global TM3 model.

Both DEHM and HANK cover the major part of the Northern Hemisphere and we assumed that the spatiotemporal pattern of the simulated CO_2 field within Europe during one month is negligibly affected by the sources and sinks outside the domain. For these two models the CO_2 concentration was therefore assumed to be constant (0 ppm) at the lateral and upper boundaries.

Also the initial conditions differ among the models. The TM3, LMDZ and DEHM models were run for the full year of 1998 and include several months of spin up (from a concentration of 0 ppm) before the July and December months that we focus on here. This is also the case for the REMO model, which is initialized with TM3 results. HANK in contrast is started up from 0 ppm on July 1st and December 1st, respectively. Preliminary tests that we made showed that the initial conditions get rapidly mixed up homogeneously over Europe within 3–5 days. Yet the results from HANK should be interpreted during the first week of each month with this caveat in mind.

In the following, the concentration fields from the five models have been referenced to the simulated monthly averaged CO_2 at Mace Head (53.33° N, 9.90 ° W) both in the maps and in the time-series plots. Here the term "referenced" means that the value at Mace Head has been subtracted in each grid cell, see Fig. 2 for a range across the models for this value. Thereby possible biases due to differences in initial conditions are minimized.

3 Results: surface distributions

In order to investigate model differences, mean simulated CO_2 distributions for July and December are displayed in Fig. 1 for all five models. Before comparing the models with each other and later with observations it is important to recognize the influence of vertical resolution, especially within the lowest few hundred meters above the ground. As seen in Table 1 the depth of the lowest model layer varies between 25 m in HANK up to 150 m in LMDZ. The simulated

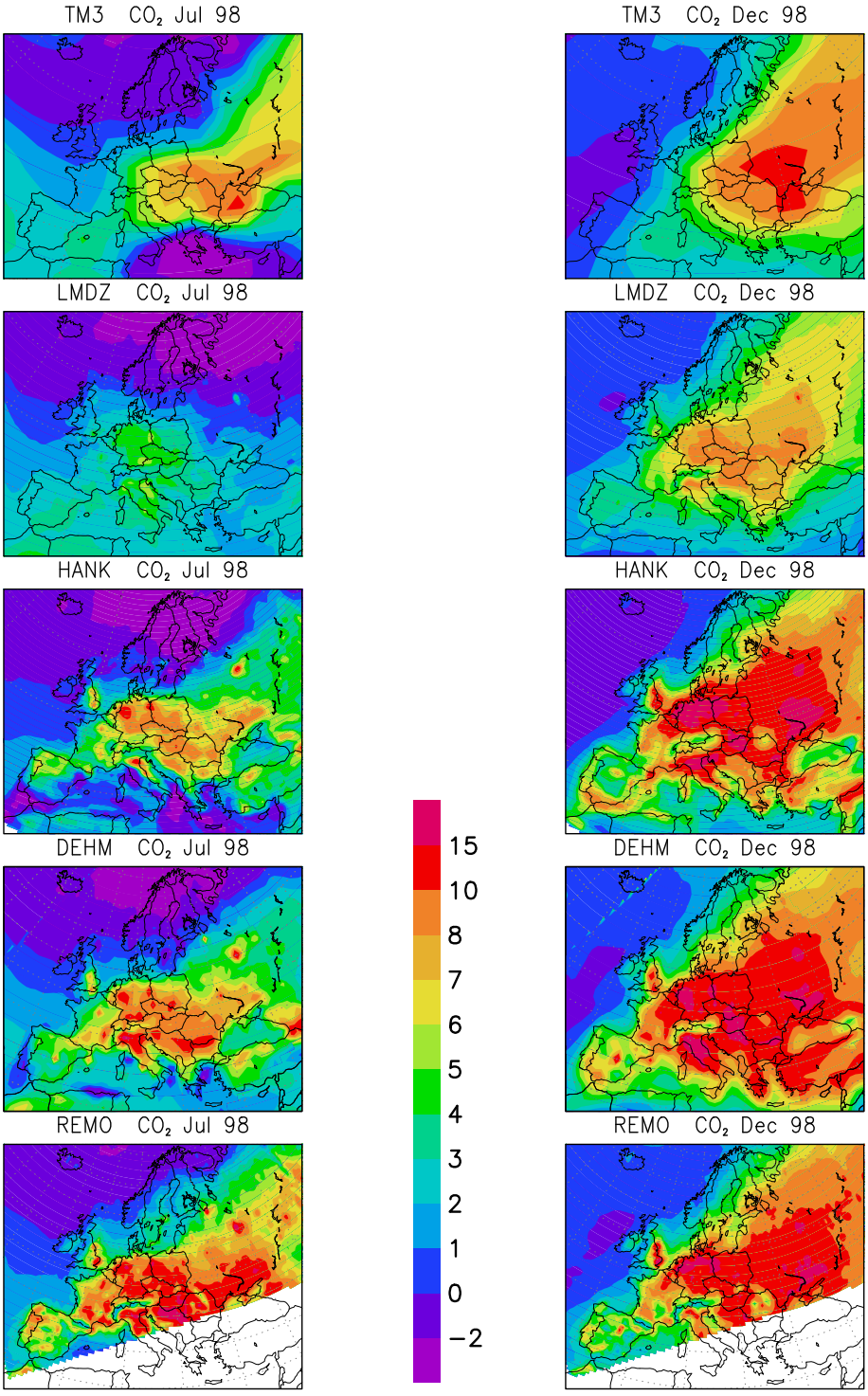

Fig. 1. Mean monthly CO_2 concentrations (in ppm) for July and December 1998, as simulated by the five transport models. Each model output has been interpolated to 11 hPa above ground and is displayed relative to the monthly CO_2 level at Mace Head, Ireland.

surface concentrations will hence represent mean CO_2 concentrations over different portions of the air column. In order to harmonize the intercomparison, each model output was interpolated to 11 hPa above ground, which is the center of the lowermost layer of the coarsest model (LMDZ).

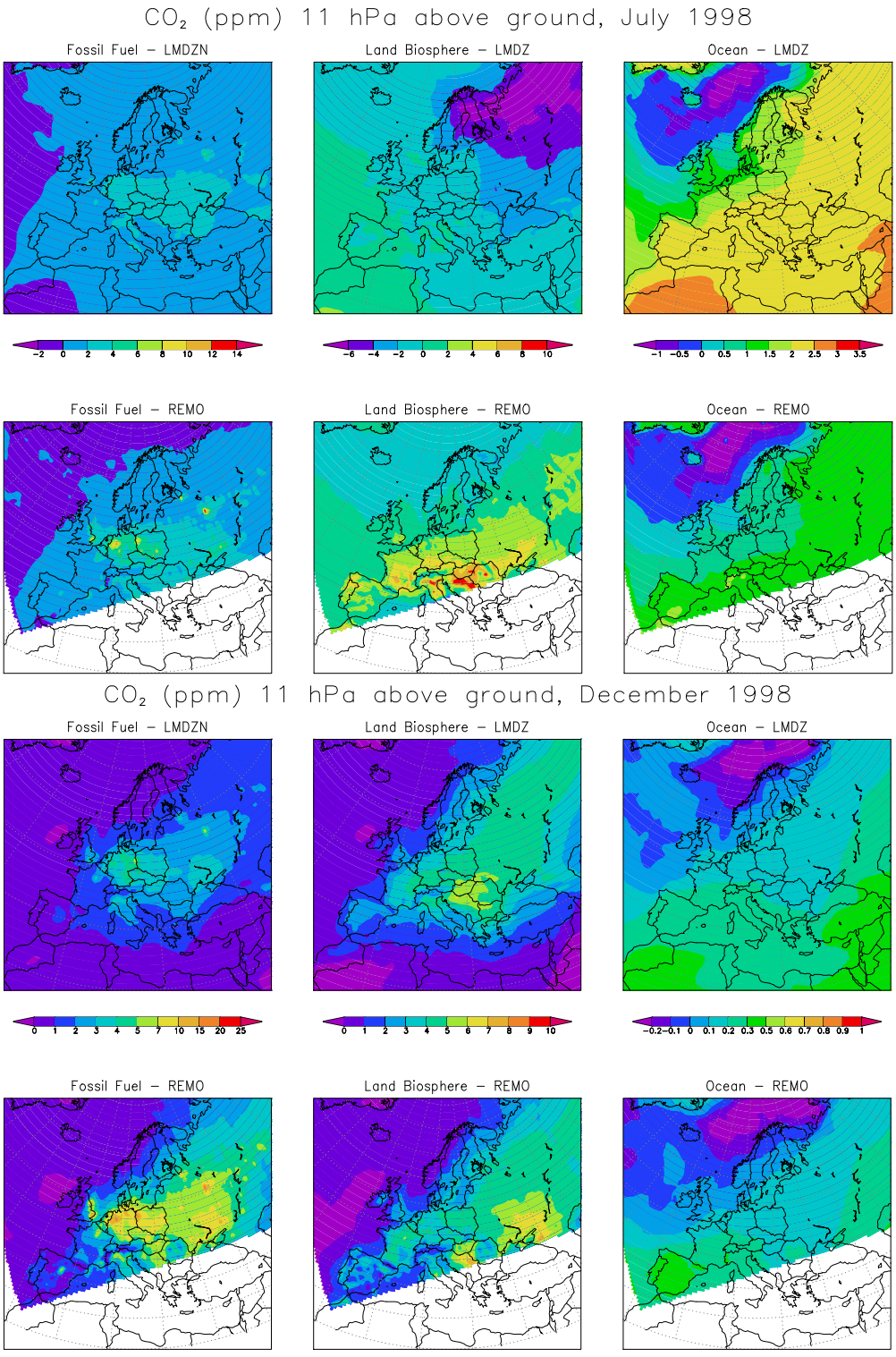

Fig. 2. The separated components for July and December, as simulated by the LMDZ and REMO models. Displayed relative to the monthly CO_2 level at Mace Head, Ireland. The level at Mace Head in July for LMDZ/REMO (in ppm): 3.0/13.2 (fossil fuel), −2.9/−4.8 (biosphere), −3.3/−5.7 (ocean) and for December: 4.7/13.8 (fossil fuel), 1.8/2.6 (biosphere), −1.5/−4.6 (ocean).

3.1 Spatial patterns for July

The overall pattern of the July monthly mean concentration field is qualitatively similar among the five models with highest CO_2 values over the continent and lower values over the Northeast Atlantic and in some of the models over the Mediterranean (Fig. 1). LMDZ seems to be an outlier with generally lower surface concentrations indicating faster boundary layer ventilation. Despite the qualitative agreement there are large quantitative differences (up to about 10 ppm). Furthermore there is a difference between coarser-resolution global model and regional model simulations: There is more fine-scale structure in the latter and there is an eastward (downstream) shift in the concentration maximum caused by fossil fuel emissions in the global models.

In order to investigate the differences between models in more detail, we show in Fig. 2 each component for July for the two most contrasting models, REMO and LMDZ.

In the simulations of fossil fuel CO_2, the impact of the heterogeneity of the emission field is evident. The increase in horizontal resolution leads to an increase in small scale features being better resolved, such as for example positive CO_2 anomalies over large cities in the regional model REMO.

The simulations of the NEE component alone indicate that the interplay between NEE and convective mixing is the main reason why total CO_2 differs among the models. In July, when the vegetation is active, alteration of near ground CO_2 varies inversely with mixing within the PBL, as shown for instance in tall tower records (Bakwin et al., 1998), global models (Denning et al., 1996) and in regional model studies (Chevillard et al., 2002b; Geels, 2003). As mixing during night is usually much less than during day, nighttime respiratory CO_2 accumulates in a shallow nocturnal boundary layer, while the low CO_2 concentrations due to photosynthesis are diluted over a deeper convective PBL during daytime. Thus even if the daily integrated CO_2 exchange between land vegetation and atmosphere is zero there will be a positive CO_2 signal at the surface. The degree to which models are able to capture this "diurnal rectification" will be discussed in more detail in Sect. 5.

The substantial difference between the global LMDZ and regional REMO simulations for the biospheric CO_2 component is mainly related to vertical mixing and vertical resolution of the models. This indicates that near-ground vertical resolution plays an important role in predicting near-ground concentrations, the realism of which will be discussed later on.

The oceanic component in both LMDZ and REMO lowers the atmospheric CO_2 content over the northern part of the Atlantic by approximately 0.5–1.0 ppm relative to Mace Head. The largest dissimilarity between the two simulations is over land where the concentration gradient is steeper in the LMDZ results.

The large differences in mean signals across model simulations and the recognition that a main cause is the difference in modeling nighttime concentrations suggest investigating alternative sampling schemes. In particular it is natural to try to take advantage of convective mixing on land during days with fair weather conditions. For such conditions near ground observations are similar to PBL concentrations (Bakwin et al., 1998) and likely as well much more homogeneous in the horizontal direction in comparison to night-time concentrations. To assess this assertion we define in the following daytime sampling as sampling restricted to the period from 10:00–17:00 Local Standard Time (LST).

As seen in Fig. 3 the difference among models in July is less dramatic for daytime averages compared to the whole-day averages shown in Fig. 1. The differences are reduced further for daytime sampling at a few hundred meters above ground (here at 40 mbar $\simeq$400 m), as seen in Fig. 3. In REMO, HANK and to some degree DEHM and LMDZ higher concentrations are seen over oceanic coastal regions during daytime for July at 11 hPa above ground. A possible explanation could be the land sea-breeze combined with the surface exchange and atmospheric mixing. Near-ground night-time air enriched in respired CO_2 is transported from land to the adjacent sea during night. Over land the night-time air enriched with CO_2 is mixed nearly homogeneously during day by convection to a height on the order of 2–3 km. Thus near ground nighttime concentrations are strongly diluted and the biosphere removes CO_2 from the PBL. Over sea the high night-time concentrations get diluted much less, as vertical mixing during day remains limited to a shallower layer and the exchange with the surface water is small. The results indicate that a model resolution of at least $1^\circ \times 1^\circ$ is needed in order to resolve this sea-breeze effect. Another distinct difference between the model results is that the Iberian Peninsula (Spain and Portugal) is not resolved well in the two global models resulting in higher near-ground concentrations in this region compared to the high-resolution models.

3.2 Spatial patterns for December

During December, the diurnal variability of atmospheric CO_2 over the European continent is much reduced compared to July, because photosynthesis and respiration are much weaker and because the day-night contrast in vertical mixing is smaller. The daytime selected and full monthly mean maps are therefore very similar and only the latter are shown (Fig. 1).

The results of the three regional models REMO, DEHM and HANK show similar concentration distributions with the same small-scale features. TM3 and LMDZ replicate the overall pattern with highest levels over central Europe, but LMDZ produces maximum accumulations near the ground that are up to 50% lower than those found in the regional models, in accordance with the simulations for July.

The CO_2 components (Fig. 2) display the overall positive CO_2 contribution from both anthropogenic sources (0.17 GtC per month in REMO) as well as respiration sources

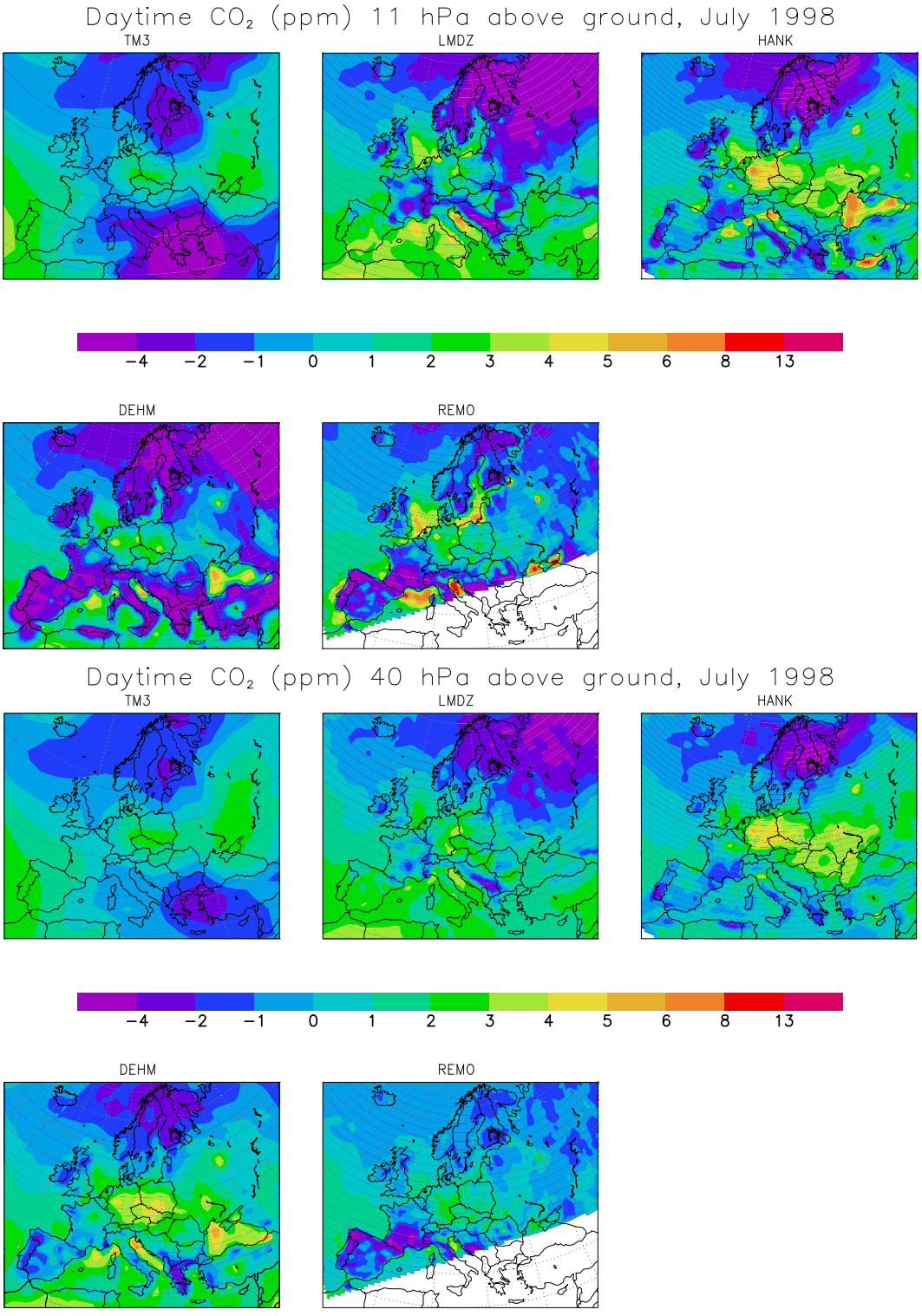

Fig. 3. Simulated mean monthly CO_2 concentrations for July based on the daytime (10:00–17:00 LST) values only at two different levels above ground. Displayed relative to the monthly CO_2 level at Mace Head, Ireland.

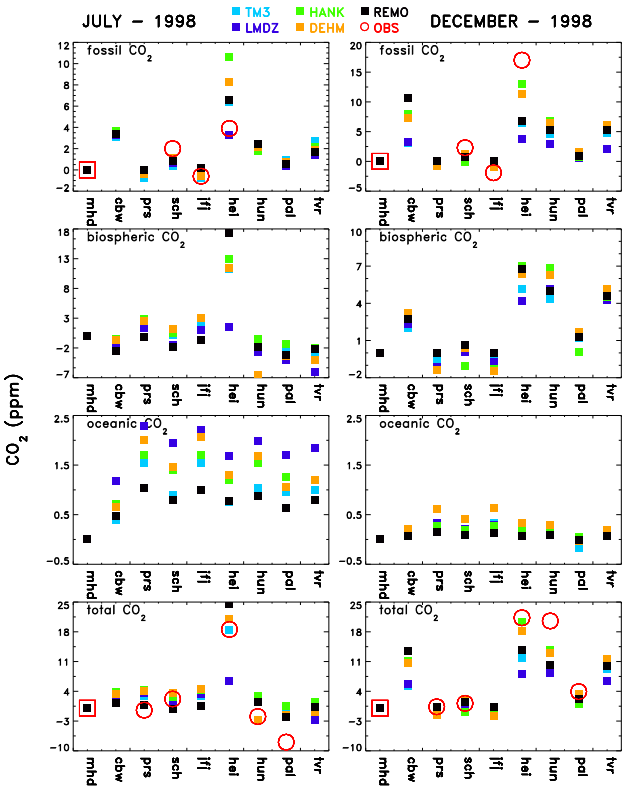

Fig. 4. The monthly averaged West to East longitudinal gradients across nine European monitoring sites displayed relative to the marine background conditions at MHD. Based on daytime values, except at HEI where nighttime data are used. Four panels are shown: 1. the fossil fuel CO_2 component as simulated and observed (based on ^{14}C observations), 2. the simulated biospheric component, 3. the simulated oceanic component, and 4. observed and simulated total CO_2. Note that for MHD ^{14}C data we have used the year 2001 as no data are available for 1998. Note also that the scales are different for each component.

(0.27 GtC for December in REMO). The fossil fuel emissions are assumed constant throughout the year, so the higher levels in December compared to July reflect the increased stability of the PBL during wintertime and the lower ventilation rate. For the NEE component the difference between summer and winter is small at some inland regions (e.g. North of the Black Sea) when using REMO. This is believed to be caused by the rectification effect and is in agreement with the damped seasonal cycle observed near the ground at continental low elevation sites (Bakwin et al., 1998). The seasonal difference will, however, depend on several model parameters and it will in particular depend on the PBL-free troposphere exchange both regarding magnitude of the exchange and the seasonal contrast. This is reflected in the modelling results based on LMDZ for which the difference between July and December is larger. The CO_2 field due to air-sea exchange is weaker in December reflecting a reduced net oceanic sink compared to July.

4 Results: horizontal and vertical gradients

4.1 Monthly averaged CO_2 gradients across Europe

Figure 4 shows the three CO_2 components as well as total CO_2 along a West-to-East transect at nine stations with latitudes in the range of 45–70° N (see Table 3 for station characteristics). Both observations (circles) and model simulations are referenced to the maritime background conditions at Mace Head (MHD), Ireland station (i.e. the MHD concentration record is subtracted from the other records). The maritime background conditions are a selective sampling of CO_2 data based on wind speed and direction as well as the standard deviation of hourly CO_2 values (Bousquet et al., 1997).

The observations have been selectively subsampled according to site-specific "regional background" criteria based on wind speed and direction. Generally for both observations and simulations only daytime values are displayed with the exception of the Heidelberg (HEI) station, an urban site, where only night-time values are sampled in order to minimize very local contamination from traffic (Levin et al., 2003). At this site model prediction for the night-time period (07:00 pm to 07:00 am LST) are therefore shown instead. Note the different scales in the individual plots in Fig. 4.

Radiocarbon ($^{14}CO_2$) measurements made on monthly integrated samples (Levin et al., 2003) give us the opportunity to evaluate the model's ability to replicate the fossil fuel CO_2 gradients across Europe. This is because CO_2 emitted by fossil fuel burning is ^{14}C free in contrast to CO_2 from all other sources. In Fig. 4 it is apparent that most models reproduce correctly an increase in the fossil fuel CO_2 component between Mace Head (MHD) and continental air measured at the Schauinsland (SCH) mountain station in Germany. But all models tend to underestimate the size of the gradient in both summer and winter. As expected, the fossil fuel CO_2 signal near the surface is much higher in December compared to July because of suppressed vertical mixing in winter. Stations that are close to large urban areas (CBW in Holland; HEI in Germany) show generally elevated concentrations compared to other stations as a result of high fossil fuel emissions nearby these locations. It is also at these two sites that we see the largest spread among the models (8–10 ppm) in December and a larger difference between observed (ca. 17 ppm at HEI relative to MHD) and simulated (between ca. 14 ppm (HANK) and ca. 4 ppm (LMDZ)) fossil fuel CO_2 gradients compared to more remote stations. This is partly because local sources influencing the Cabauw and Heidelberg stations are not resolved in the EDGAR global emission product ($1^\circ \times 1^\circ$ resolution). In addition there are site representativeness issues, which further complicate the data-simulation comparison. It is also important to remember that the comparison at Heidelberg includes night time data and the large differences could therefore partly reflect the model's differences in predicting local night time conditions.

Table 3. A few site characteristics, corresponding to the included monitoring sites for atmospheric CO_2. In Figs. 7, 9, 10 and 11 the observed values are characterized as background (Obs. Bg) or non-background (Obs. NBg) values depending on which type of air mass they are assumed to represent.

Site	Code	Location	Altitude a.s.l.	Type	Characteristics
Mace Head	MHD	53.33° N, 9.90° W	5 m	Continuous	Coastal site
Cabauw	CBW	51.97° N,4.92° E	0 m	Continuous	Tower
Plateau Rosa	PRS	45.93° N,7.70° E	3482 m	Continuous	Mountain site
Schauinsland	SCH	47.92° N, 7.92° E	1205 m	Continuous	Mountain site
Jungfraujoch	JFJ	46.55° N, 7.98° E	3580 m	Flask	Mountain site
Heidelberg	HEI	49.40° N,8.70° E	116 m	Continuous	Low alt., western Europe, urban
Hegyhatsal	HUN	46.95° N, 16.65° E	248 m	Continuous	Continental tower
Pallas	PAL	67.97° N, 24.12° E	560 m	Continuous	Continental hill site
Tver	TVR	56.47° N, 32.92° E	265 m	Continuous	Continental tower
Monte Cimone	CMN	44.20° N, 10.70° E	2165 m	Continuous	Mountain site

In July all models predict the same fossil CO_2 contribution ($\pm$1 ppm) across Europe, except at Heidelberg where the difference in-between models again is large and the observed levels are overestimated except by the LMDZ model. This overestimation could indicate that the included fossil fuel emissions are too large in this region in summer.

In December the simulated biospheric CO_2 component is generally higher in the interior of the continent than close to the coast. This is because respiratory CO_2 is progressively accumulating along the main air-flow directed on average from the Atlantic to the continent. In July, day-time biotic CO_2 is lower over land due to photosynthesis. Exceptions are the alpine high-altitude sites Plateau Rosa (PRS) and Jungfraujoch (JFJ) where CO_2 respired during previous nights can be uplifted by daytime convective mixing, leading to a positive CO_2 signal compared to Mace Head. At most sites a larger spread amongst the models is generally seen for the biotic signal compared to the other CO_2 components, and this spread is enhanced during summer. This is a reflection of different strengths of the diurnal mixing in the models (see also Fig. 2).

The modelled oceanic component of CO_2 shows a weaker signal and less spread than the other components both during summer and winter (note the differences in the scales in Fig. 4). Relatively small longitudinal gradients ($<$2.5 ppm) are seen for this component and the gradient tend to be most pronounced in LMDZ in July. In December the corresponding gradients are quite similar in the model results.

In December the West-East gradient of the total CO_2 signal across the stations is captured within $\pm$4 ppm at three (PRS, SCH, PAL) out of five stations with observations, while the high levels at HEI and HUN are underestimated by nearly all models. In contrast, most models underestimate the negative CO_2 difference between the Mace Head and central and northern regions of Europe (e.g. the Finnish station Pallas (PAL)) in July. Based on the evaluation of ^{222}Rn (see Vermeulen et al., in preparation) and the fossil fuel component, we attribute this bias to the NEE component. The maximum drawdown in the TURC NEE fluxes occurs about one month too early and the uptake in July is thereby underestimated. By assuming that the biosphere is in balance on a yearly basis (see Sect. 2.2), we also neglect the terrestrial sink of the Northern Hemisphere, which may lead to an underestimation of the biospheric summer uptake and hence could explain the simulated underestimation of the westward depletion of CO_2 across Europe.

4.2 Vertical profiles of CO_2 through July and December

Vertical CO_2 profile observations from Orleans, France provide a constraint on model simulation of vertical air exchange. The observations are from approximately weekly sampled flasks filled onboard an aircraft at 500, 1500, 2500 and 3500 m above ground The observations are taken during fair weather conditions around mid-day. We selected the model output for afternoon concentrations, but not for fair weather conditions. An arbitrary reference value of 360 ppm is subtracted from the observations. Figure 5 shows that the observed CO_2 increases with height during summer and decreases with height during winter. All the models capture qualitatively these gradients, but the modeled summer-winter contrast tends to be too large.

The figure shows that below 500 m, and hence below the lowest observation level, the models diverge strongly. Higher resolution models predict considerably higher concentrations at the surface in winter compared to the coarser resolution global models. The error bars show the monthly standard deviation for one regional model (DEHM) and one global model (LMDZ). They indicate that the variability of regional models increases greatly closer to the surface compared to global models, in accordance with the time series evaluation discussed in the following.

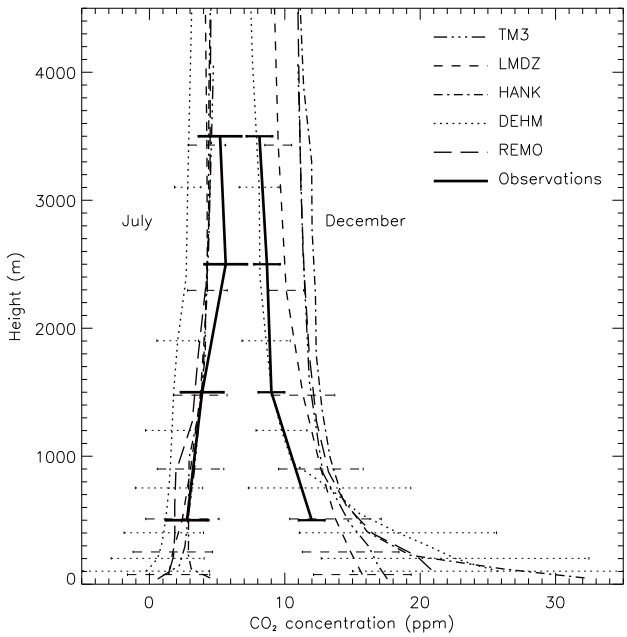

Fig. 5. Monthly mean observed and simulated vertical profiles for July and December at Orleans (48.83° N, 2.50° E), France. The observed curves are based on weekly flask measurements sampled onboard an aircraft and then averaged at 500, 1500, 2500 and 3500 m above ground. A value of 360 ppm has been subtracted from the observations. The simulated curves are based on daytime values. Error bars are shown for the observations as well as for the DEHM and LMDZ model in order to display the standard deviation of the predicted concentrations at the different heights.

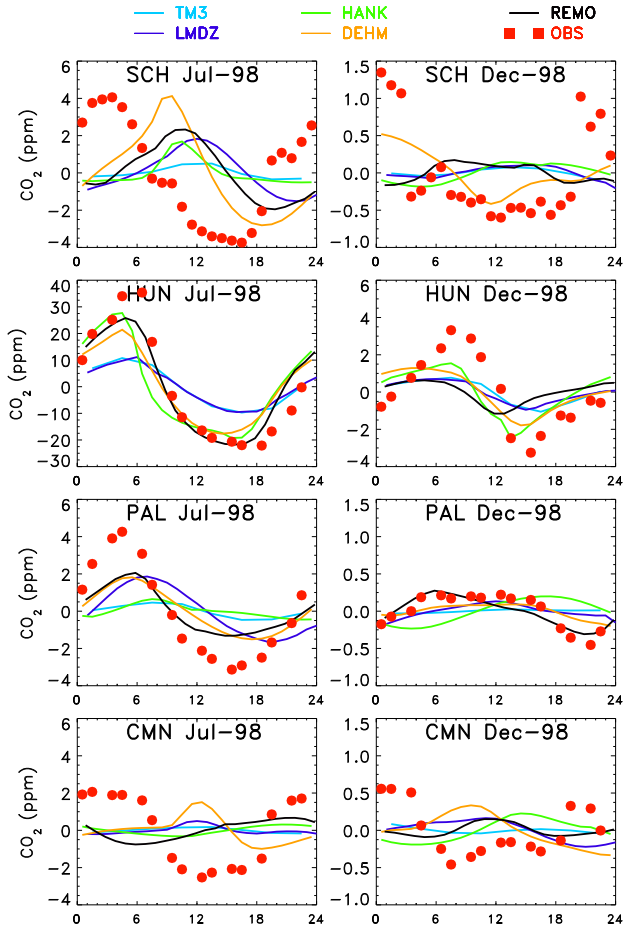

Fig. 6. Observed and simulated mean diurnal cycle (UTC) at four monitoring sites in Europe (see Table 3 for a short description of the different sites). Based on hourly values from July and December 1998.

5 Results: time series and statistical evaluation

Due to local sources, variations in PBL depth and topographic characteristics, the observations at a given station may not be spatially representative of an area large enough to be comparable to the resolution of the models. As shown by Gerbig et al. (2003) this representation error increases significantly with the horizontal averaging distance (or model grid size). This is important to bear in mind, in the following data-model comparisons including continuous data on land (see the list of stations in Table 3).

For the comparisons each model output has been sampled at each station and averaged on an hourly basis. In the vertical, modeled concentrations are linearly interpolated to the station altitudes.

5.1 Time series for July

During July, the uptake of CO_2 as well as the diurnal PBL height are close to their annual maximum over Europe. An important question is to what extent models differ among each other for representing the diurnal cycle of CO_2 which dominates the short-term variability. For all stations, models show a common tendency to underestimate the amplitude of the CO_2 diurnal cycle. We illustrate this in Fig. 6 by comparing the predicted and observed mean diurnal cycle at two mid- to high-elevation mountain stations (SCH and CMN; resp. at 1205 m a.s.l. and 2165 m a.s.l.) and two lower elevation stations (HUN and PAL; resp. in Western Hungary and Northern Finland). The Hungarian station is a tower with measurements from four levels. Here we include the data from the 115 m level, as the lower levels are more sensitive to local sources that are not well represented in the model grids used in this study.

Both HUN and PAL sites in Fig. 6 show a large spread amongst models for the diurnal amplitude of CO_2, ranging from 18 to 45 ppm at HUN (observed amplitude is ∼60 ppm) and from 1 to 9 ppm at PAL (observed amplitude is ∼7 ppm). All models produce an increase in concentration starting at sunset when PBL convection stops, and lasting until photosynthesis begins again in the next morning at around 07:00

to 08:00 LST. At the Hungarian site (HUN), all models are nicely in phase with observations, but REMO, DEHM and HANK underestimate the diurnal amplitude by a factor of 1.2 to 1.5, while LMDZ and TM3 underestimate it by roughly a factor of 3. At Pallas (PAL) the difference between mesoscale models and global models is less clear. In general the models underestimate the observed diurnal cycle by a factor of ∼2–7. This is not surprising since the prescribed TURC flux (see Sect. 2.2) is known to underestimate the NEE diurnal cycle amplitude at high latitudes compared to eddy-flux tower measurements (Aalto et al., 2004).

The CO_2 diurnal variation reflects the day-night contrast both in NEE and in PBL vertical mixing and its variability. As the same set of surface fluxes are being used in all the models, differences between models must reflect differences in vertical/horizontal mixing. The importance of the vertical resolution within the PBL is evident in the LMDZ simulations at the low altitude site HUN, where the diurnal cycle is underestimated. Over Europe the horizontal resolution is about the same as in HANK, but the vertical resolution of the PBL is lower (4 levels below 1500 m against 10 i HANK) and the parametrization of turbulent diffusion is different. For TM3 the coarser horizontal resolution of the fluxes can be part of the explanation for the smooth diurnal signal seen for this model.

Besides the biosphere-atmosphere exchange fluxes diurnal changes in vertical mixing also cause a diurnal variation in the fossil fuel component, on the order of up to 3 ppm at low altitude stations close to regional fossil emissions, like HUN. In contrast, diurnal vertical mixing acting on the oceanic CO_2 component contributes negligibly to the observed signals (e.g. <0.1 ppm at HUN).

Figure 7 illustrates the hourly variability of CO_2 throughout the month of July. It is seen again that none of the models are able to reproduce the very high CO_2 mixing ratios observed during some nights for the same reasons discussed earlier on.

At mountain stations SCH and CMN, all models simulate diurnal cycles in CO_2 in July as for lower altitude sites, but smaller in amplitude with 0.5 to 7 ppm for SCH and 0.5 to 2.5 ppm for CMN (Figs. 6 and 7). The timing of the diurnal cycle is shifted by a few hours compared to low elevation stations, with both an earlier nighttime maximum and daytime minimum. As seen in both Figures the models underestimate the observed amplitude of the diurnal cycle at CMN (∼4.5 ppm) and SCH (∼7 ppm), and are out of phase with the observations. At CMN, all models are opposite in phase with the observations, producing a maximum of CO_2 at mid-day. We attribute such deviations to the fact that the mountain stations in the real world are more directly connected to surface sources by local thermally-induced circulations (upslope winds over sunlit slopes) during the day than predicted in a model with smooth topography. In the current study we also sample the model output at the elevation (a.s.l.) corresponding to the actual elevation of each site, i.e.

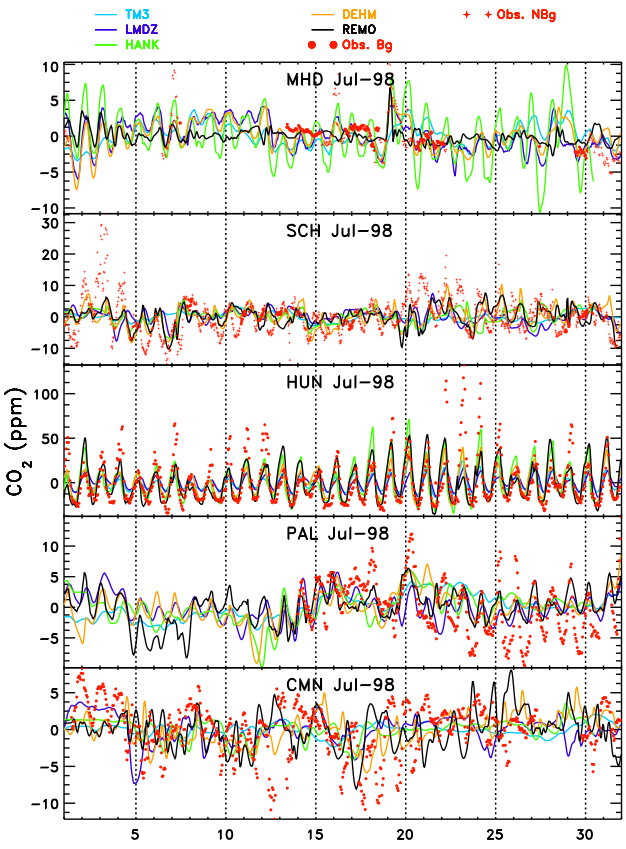

Fig. 7. Observed and simulated hourly time series for July 1998. At five different monitoring sites in Europe (see Table 3).

at some higher model level. Therefore, in most mountain regions the CO_2 signal at a given station is in the models more decoupled from the ground than in reality because the real elevation of the site is much higher than the model topography. The lagged predicted diurnal signal is then induced by the diurnal cycle at the surface propagating up through the convective PBL in the model. An exemplification of this effect can be seen in Fig. 8 where the observed diurnal cycle at CMN (2165 m a.s.l.) is compared to the REMO output for July. When plotting the CO_2 values at several model layers, it is clear that the values at the model layer corresponding to the true height of the station (the sixth layer at 1743 m a.s.l.) is out of phase with the observed diurnal cycle. The agreement between model predictions and observations increases closer to the surface and the results from the fourth model layer (1090 m a.s.l. and 529 m above ground) captures the diurnal cycle much better. It is thus apparent that representation of mountain stations is an important issue that needs to be addressed, when such data are included in atmospheric inversions (e.g. Peylin et al., 2005).

The hourly data shown in Fig. 7, nevertheless indicate that the models are able to capture most of the synoptic scale

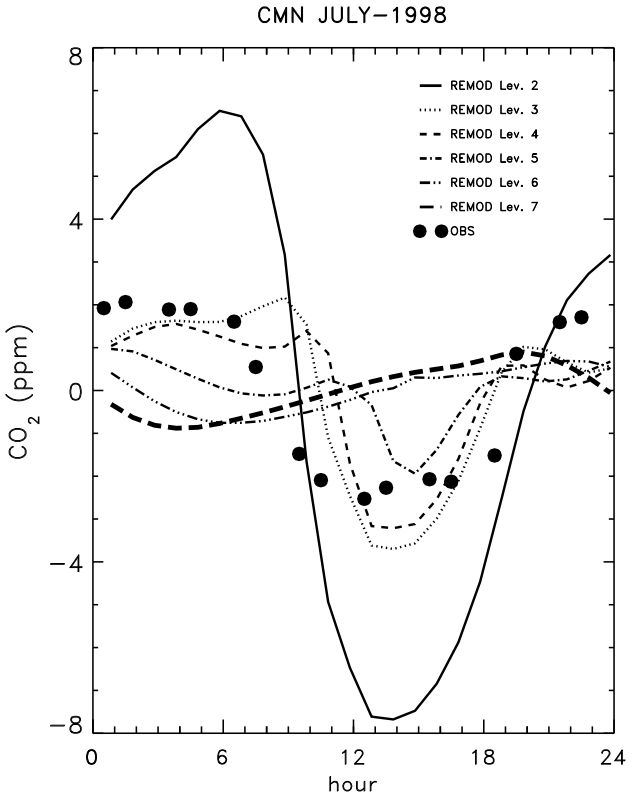

Fig. 8. Mean diurnal cycle for July as simulated by the REMO model and observed at the mountain site Monte Cimone (2165 m a.s.l.) in Italy. The model results are shown for the lowest six levels just above the surface layer.

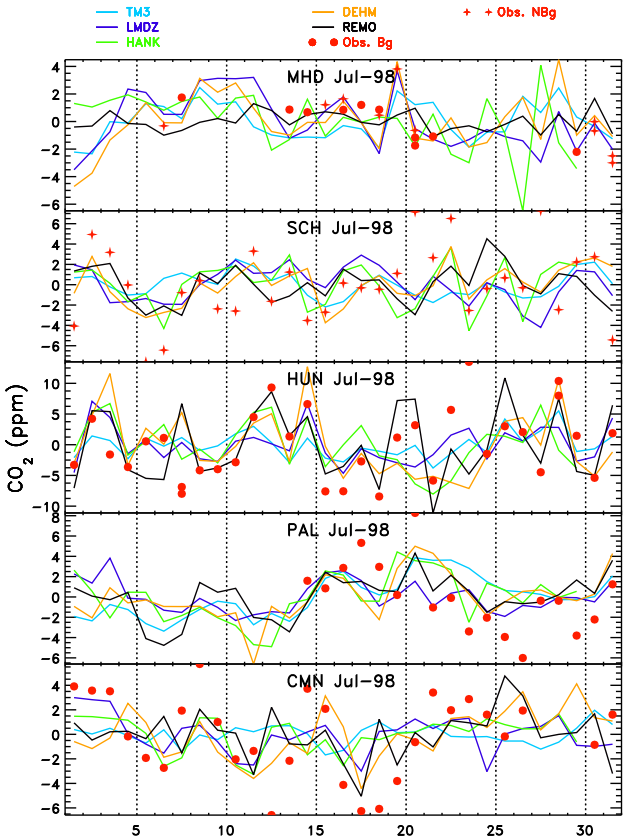

Fig. 9. Daily averaged time series based on daytime selected values in July 1998.

variability leading e.g. to day-to-day changes in the amplitude of the diurnal cycle. These changes are mainly caused by synoptic variability in atmospheric transport processes coupled with synoptic changes in NEE. As an example, for the night of 7–8 July at the low altitude Hungarian station (HUN), there was no observed build up of CO_2 after two consecutive nights with high CO_2 accumulations. This "event" correctly reproduced in all models is explained by the passage of a front during 7–9 July that broke down the stability of the nocturnal PBL.

However, the large differences between models at the hourly time scale suggest to average the measurements, for instance over the mid-day period, when convection is (generally) well developed and the CO_2 variability is small. The new question raised here is then the ability and robustness of transport models to capture the day-to-day changes in daytime CO_2, related to transport on synoptic time scales and containing information on the underlying source/sink processes. We show in Fig. 9 the day-time (10:00–17:00 LST) averaged data and model results at five stations (Table 3). Overall, all models capture the timing of most day-to-day changes, but they still show significant differences in the predicted magnitude. This suggests that while horizontal synoptic transport is realistic and similar both using mesoscale and global models the vertical transport is markedly different among the models.

Each station also has specific characteristics, which can be used to constrain different aspects of the transport models. The CO_2 record at Mace Head shows very stable (± 0.3 ppm) marine "baseline" CO_2 values under westerly wind conditions (13–18 July except 16 July, in Fig. 9) when reached by oceanic air masses, over which continental air masses deliver CO_2 maxima and minima (Bousquet et al., 1997). This is fairly well reproduced in most of the models, but with a larger amplitude (± 0.5 to ± 1.0 ppm). At the continental location in Central Europe (HUN) a larger observed and modelled CO_2 variability (by a factor of around 2) caused by synoptic systems is seen compared to mountain or coastal stations. All models roughly capture this feature.

5.2 Time series for December

The averaged diurnal cycle, hourly time series and daytime selected means for December are displayed in Figs. 6, 10 and 11, respectively. In general, on an hourly basis, the

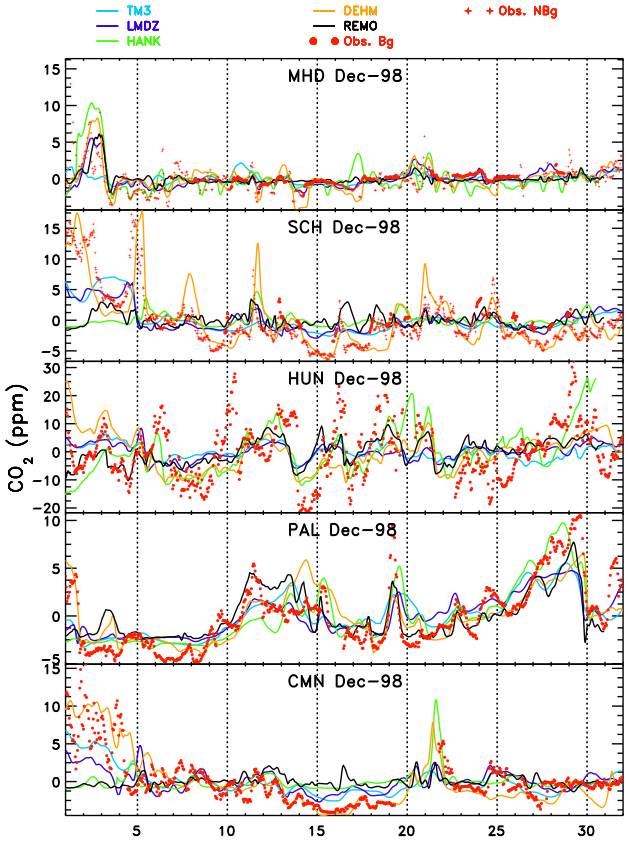

Fig. 10. Observed and simulated hourly time series for December 1998.

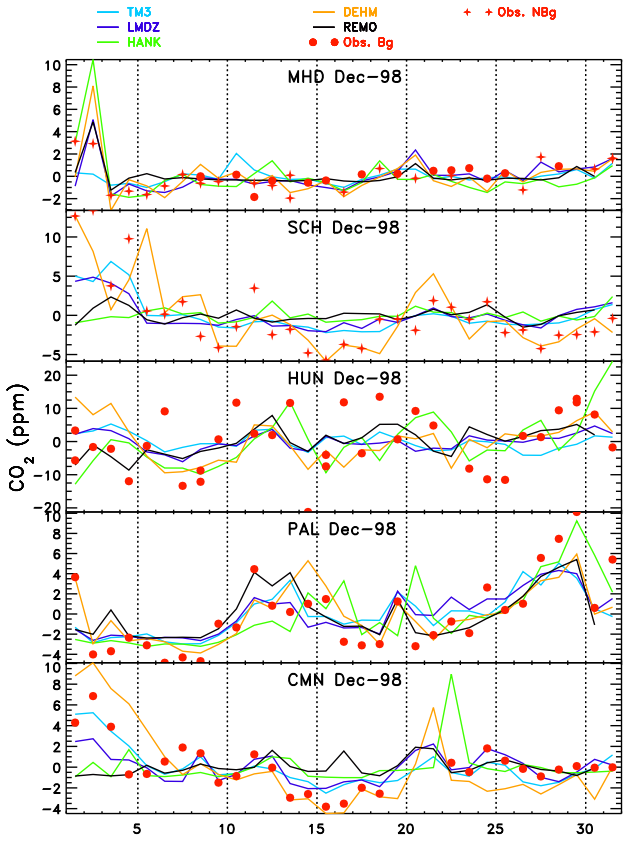

Fig. 11. Daily averaged time series based on daytime selected values in December 1998.

agreement between models and between models and observations is much higher in December compared to July. Outside the photosynthetically active period, soils in temperate and northern Europe respire CO_2 almost uniformly throughout the day, resulting in a small biospheric CO_2 diurnal cycle (e.g. Aurela et al., 2001). Further south, where photosynthesis persists, the amplitude of the diurnal NEE is also smaller than in summer (e.g. Kowalski et al., 2003). Generally, low-pressure systems are more frequent and intense in winter than in summer due to the larger temperature contrasts between the continents and the ocean. They form over the North Atlantic before they move in a westerly flow over the continent each 3–5 days. Besides, as seen in Figs. 1 and 4, day-time mixing is inhibited in December, which has the effect to accumulate CO_2 in the boundary layer (e.g. Levin et al., 1995; Haszpra, 1999), a phenomenon also observed for other anthropogenic pollutants.

We note the occurrence at HUN of periods of a few days during which CO_2 is very high (10 to 20 ppm above the marine background). This station is located in the Carpathian Basin, surrounded by a ring of mountains. Anticyclonic conditions can during winter lead to trapping of cold air in this basin and hence very high surface concentrations of CO_2. Likewise, two periods with a gradual near surface CO_2 accumulation of about 5–10 ppm within 2–4 days is observed at PAL in Finland. At MHD, there is one "pollution" episode of European origin with CO_2 rising by up to about 8 ppm above the marine baseline in early December. This episode is associated with a high pressure system developed just west of Ireland. Also at the more high elevation sites (CMN and SCH) episodes with CO_2 levels above 10 ppm are seen during December.

5.3 Statistical evaluation

In order to obtain a more quantitative measure of the models' ability to capture the observed variability, a statistical evaluation is carried out at five European sites. So-called Taylor diagrams (Taylor, 2001), displaying both relative standard deviation, relative root-mean-square difference and the correlation between observed and simulated time series, are used here. These statistics can be used to highlight how much of the overall root-mean-square difference is related to differences in variance and how much is due to poor correlation between models and observations. In the Taylor diagram, the relative standard deviation, defined as the simulated standard

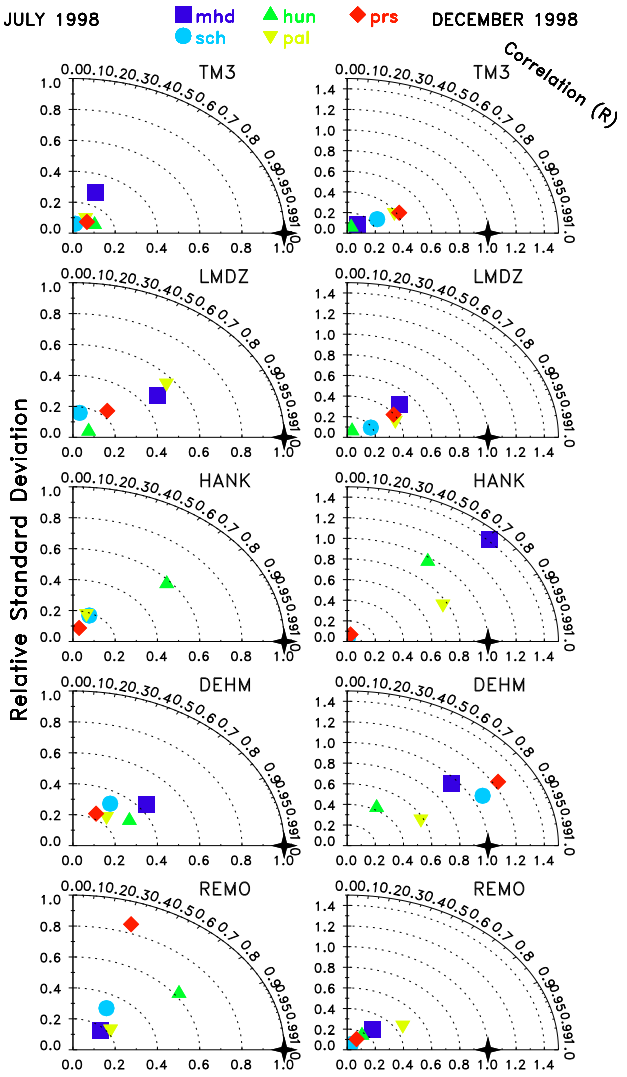

Fig. 12. Taylor diagram collecting the relative standard deviation, relative RMS difference and the correlation coefficient between observed and simulated time series of CO_2 during the month of July and December 1998. The statistics are based on hourly data from five European locations and the five models. For HANK the result at MHD is off the scale with a relative standard deviation of 2.22 and a correlation coefficient of 0.77.

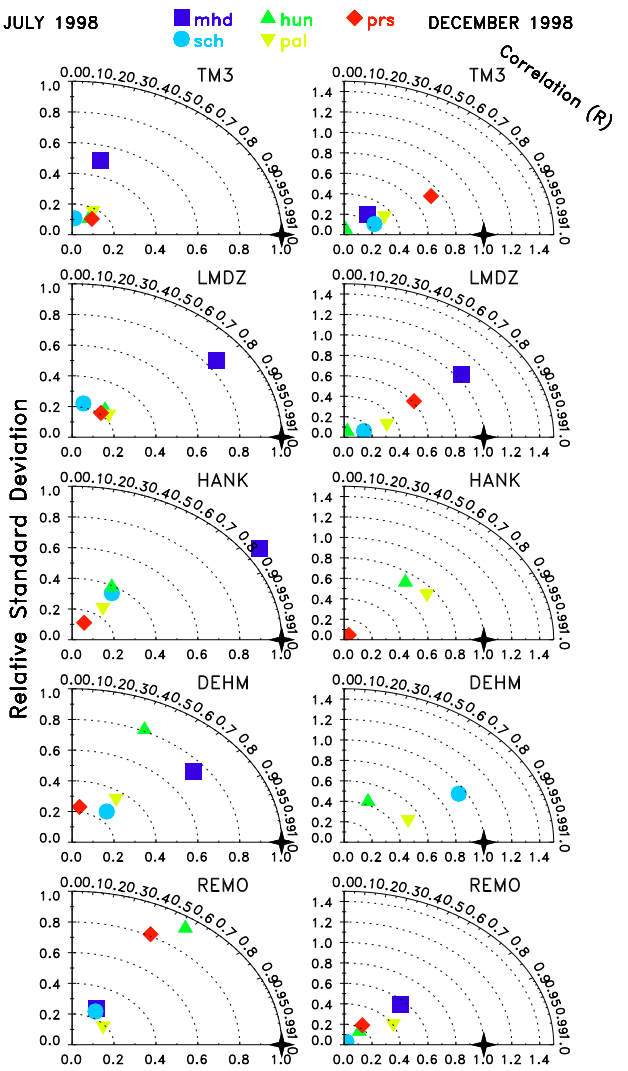

Fig. 13. Taylor diagram collecting the relative standard deviation, relative RMS difference and the correlation coefficient between observed and simulated time series of CO_2 during the month of July and December 1998. The statistics are based on daily mean values based on daytime selected data from five European locations and the five models. For HANK the result at MHD is off the scale with a relative standard deviation of 2.81 and a correlation coefficient of 0.79. The same is true for DEHM at MHD/PRS with a standard deviation of 2.07/2.09 and a correlation of 0.78/0.85.

deviation along time divided by the observed one, is plotted as radial distance from the origin. The cosine of the angle with respect to the horizontal axis equals the correlation coefficient. A (hypothetical) model in perfect agreement with observations would be located where the circle with radius equal to unity intersect the x-axis (indicated as a star in the plot). The Taylor diagram has the property that the distance between an actual model result and the reference point of the perfect model (the star) equals the relative root mean square error (RMS). In Fig. 12, Taylor diagrams have been calculated from all hourly data, while Fig. 13 is calculated from daily mean concentrations based on day-time selected values.

Comparing the statistics of hourly data (strongly influenced by the diurnal cycle, at least in summer) and of daytime selected daily means (expected to reflect synoptic variability), the picture turns out to be broadly similar. Modelled standard deviations are generally larger for the daily means, in particular at the coastal site Mace Head (MHD) and the mountain site Plateau Rosa (PRS). Correlation

coefficients are similar between hourly and daily for most stations/models.

As expected from the time series analysis above, all the models underestimate the variability during summer, with a tendency towards smaller normalized standard deviation for coarser-resolution models. Plateau Rosa (PRS) and Schauinsland (SCH) often show poorer correlations than the other sites, in accordance with the before-mentioned difficulties for properly locating mountain sites in models.

In December, when diurnal cycles are small, the model-data correlations are slightly higher than in July, as the phase of the synoptic variability is reasonably captured by all models. However, the size of individual high CO_2 events is mostly still underestimated, especially by the two global models, and by REMO (the latter maybe because of the use of boundary conditions based on simulations with the global model TM3). Nevertheless, overestimation occurs as well. When compared to observations, the DEHM model shows a high correlation (>0.65) at four sites as well as a relative standard deviation around one and a small RMS. The standard deviation of HANK is also reasonable for MHD and HUN, while it is greatly underestimated at the mountain stations PRS and SCH.

6 Summary and conclusions

We have tested model behavior for simulating lower tropospheric CO_2 across Europe using one set of surface fluxes and five atmospheric transport models with different horizontal and vertical resolution. Model predictions are confronted with new continuous and discrete CO_2 and $^{14}CO_2$ atmospheric concentrations measured for the purpose of estimating the carbon balance of Europe using an atmospheric approach. A main purpose of the study is to learn how to combine continental data and models for flux estimation purpose given the complex nature of lower troposphere CO_2 above the continents. The results show that the spread of predicted CO_2 across the models is large (up to 10 ppm for the monthly mean distribution). From the separated components (biosphere, ocean and fossil fuel) it is evident that these differences are not only linked to the horizontal resolution of the models, but also to a large degree to the representation of mixing within the boundary layer and the vertical resolution of the models. The spread is reduced when restricting sampling to the afternoon. It is further reduced when sampling a few hundred meters above ground.

Main conclusions and recommendations resulting from the study for constraining land carbon sources and sinks using high-resolution concentration data and state-of-the art transport models through inverse methods are given in the following:

1) At high-altitude stations both coarse and high-resolution models employed fail to reproduce phasing of daily cycles as well as absolute concentrations observed due to an insufficient representation of the surface topography. Furthermore, the flow fields around mountainous sites are extremely difficult to simulate and therefore the transport patterns from the source areas to the mountain site are difficult to catch. The recommendation is therefore that low altitude stations presently are preferable in inverse studies. If high altitude stations are used then the model level that represents the specific sites should be applied.

2) The modelled height of the PBL has substantial influence on the concentration levels. This parameter is nevertheless very difficult to simulate correctly and this is one of the main sources of uncertainties in transport models. The model-surface data comparisons show a large spread, with the observed diurnal cycle being underestimated by up to a factor of 1.5 for the regional models and up to a factor of 3 for global models at a low altitude continental site in Hungary. Especially during night time the height of the PBL can be uncertain with several hundred percent, and from the hourly time series it is evident that the models underestimate the night-time concentrations. During day time the PBL height is better resolved by the models and hence less uncertain. Furthermore the parameterizations of the PBL height are mainly designed for day time applications. The recommendation is therefore that at low altitude sites only the afternoon values of concentrations can be represented sufficiently well by current models and therefore afternoon values are more appropriate for constraining large-scale sources and sinks in combination with transport models.

3) The vertical CO_2 profile is difficult to simulate, especially near the ground due to the surface exchange. Even when using only afternoon values it is clear that data sampled several hundred meters above ground can be represented substantially more robust in the models. The recommendation is therefore to emphasize the use of tower data in inverse studies.

4) The traditional coarse resolution transport models are too coarse to resolve not only fine-scale features associated with fossil fuel emissions, but also larger-scale features like the concentration distribution above the south-western Europe. Our results indicate that a horizontal resolution of max. $1^\circ \times 1^\circ$ combined with a vertical resolution of max. 100 m for the lowest layer, should be able to capture such distributions. The recommendation is therefore to use higher resolution models in future studies including continental data.

It is important to note that both high altitude sites and hourly data in general include important information about the carbon cycle that could be valuable in budget studies. But in order to include such data in studies with the current generation models a detailed assessment of model capability needs to be carried out for each site, preferable in cooperation with the people responsible for the monitoring network.

Acknowledgements. The work has been done within the framework of the EU cluster project CARBOEUROPE, sub-project AEROCARB (Airborne European Regional Observations of the

Carbon Balance). We thank the participants of AEROCARB for useful discussions and for making their observations available for this study. Especially warm thanks to I. Levin for her thoughtful comments to this work. The project was funded by the European Commission under contract no. EVK2-CT-1999-00013.

Edited by: W. E. Asher

References

Aalto, T., Hatakka, J., Paatero, J., Tuovinen, J.-P., Aurela, M., Laurila, T., Holmén, K., Trivett, N., and Viisanen, Y.: Tropospheric carbon dioxide concentrations at a northern boreal site in Finland: basic variations and source areas, Tellus, 54B, 110–126, 2002.

Aalto, T., Ciais, P., Chevillard, A., and Moulin, C.: Optimal determination of the parameters controlling biospheric CO_2 fluxes over Europe using eddy covariance fluxes and NDVI measurements, Tellus, 56B, 93–104, 2004.

Apadula, F., Gotti, A., Pigini, A., Longhetto, A., Rocchetti, F., Cassardo, C., Ferrarese, S., and Forza, R.: Localization of source and sink regions of carbon dioxide through the method of the synoptic air trajectory statistics, Atmos. Environ., 37, 3757–3770, 2003.

Aurela, M., Laurila, T., and Touvinen, J.-P.: Seasonal CO_2 balances of a subarctic mire, J. Geophys. Res., 106, 1623–1637.

Bakwin, P. S., Tans, P. P., Hurst, D. F., and Zhao, C.: Measurements of carbon dioxide on very tall towers: results of the NOAA/CMDL program, Tellus, 50B, 401–415, 1998.

Blasing T. J., Broniak, C. T., Marland, G.: The annual cycle of fossil-fuel carbon dioxide emissions in the United States, Tellus, 57B, 107–115, 2005.

Bousquet, P., Ciais, P., Monfray, P., Balkanski, Y., and Ramonet, M.: Influence of two atmospheric transport models on inferring sources and sinks of atmospheric CO_2, Tellus, 48B, 568–582, 1996.

Bousquet, P., Gaudry, A., Ciais, P., Kazan, V. P., Monfray, P., Simmonds, P. G., Jennings, S. G., and O'Connor, T. C.: Atmospheric concentration variations recorded at Mace Head, Ireland from 1992 to 1994, Phys. Chem. Earth, 21, 5-6, 477–481, 1997.

Bousquet, P., Peylin, P. Ciais, P., Le Quéré, C., Friedlingstein, P., and Tans, P. P.: Regional changes in carbon dioxide fluxes of land and oceans since 1980, Science, 260, 1342–1346, 2000.

Chevillard, A.: Etude a haute resolution du CO_2 atmospherique en Europe et en Siberie, Impact pour les bilans de carbone, PhD Thesis, Universite Pierre et Marie Curie, Paris, France, 2001.

Chevillard, A., Ciais, P., Karstens, U., Heimann, M., Schmidt, M., Levin, I., Jacob, D., and Podzun, R.: Transport of ^{222}Rn using the regional model REMO, A detailed comparison with measurements over Europe, Tellus, 54B, 872–894, 2002a.

Chevillard A., Karstens, U., Ciais, P., Lafont, S., and Heimann, M.: Simulation of atmospheric CO_2 over Europe and Western Siberia using the regional scale model REMO, Tellus, 54B, 872–894, 2002b.

Christensen, J. H.: The Danish Eulerian hemispheric model - a three-dimensional air pollution model used for the arctic, Atmos. Environ., 31, 4169–4191, 1997.

Christensen, J., Brandt, J., Frohn, L. M., and Skov, H.: Modelling of Mercury in the Arctic with the Danish Eulerian Hemispheric Model, Atmos. Chem. Phys., 4, 2251–2257, 2004, http://www.atmos-chem-phys.net/4/2251/2004/.

Denning, A. S., Randall, D. A., Collatz, G. J., and Sellers, P. J.: Simulations of terrestrial carbon metabolism and atmospheric CO_2 in a general circulation model, Part 2: Simulated CO_2 concentrations, Tellus, 48B, 8543–8567, 1996.

Fan S., Gloor, M., Mahlman, J., Pacala, S., Sarmiento, J., Takahashi T., and Tans, P.: A large terrestrial carbon sink in North America implied by atmospheric and oceanic carbon dioxide data and models, Science, 282, 442–446, 1998.

Frohn, L. M., Christensen, J. H., and Brandt J.: Development of a high resolution nested air pollution model – the numerical approach, J. Comput. Phys., 179(1), 68–94, 2002.

Frohn, L. M.: A study of long-term high-resolution air pollution modelling, PhD thesis, National Environmental Research Institute, Department of Atmospheric Environment, Denmark, 2004.

Fung, I. Y., Tucker, C. J., and Prentice, K. C.: Application of advanced very high resolution radiometer vegetation index to study atmosphere-biosphere exchange of CO_2, J. Geophys. Res., 92(D3), 2999–3015, 1987.

Geels, C.: Simulating the current CO_2 content of the atmosphere: Including surface fluxes and transport across the Northern Hemisphere, PhD thesis, National Environmental Research Institute, Department of Atmospheric Environment, Denmark, 2003.

Geels, C., Doney, S. C., Dargaville, R., Brandt J., and Christensen, J. H.: Investigating the sources of synoptic variability in atmospheric CO_2 measurements over the Northern Hemisphere continents – a regional model study, Tellus, 56B, 35–50, 2004.

Gerbig, C., Lin, J. C, Wofsy, S. C., Daube, B. C., Andrews, A. E., Stephens, B. B., Bakwin, P. S., and Grainger, C. A.: Towards constraining regional-scale fluxes of CO_2 with atmospheric observations over a continent: 1. Observed spatial variability from airborne platforms, J. Geophys. Res., 108(D24), 4756, doi:10.1029/2002JD003018, 2003.

Gloor, M., Fung, S. M., and Sarmiento, J.: Optimal sampling of the atmosphere for purpose of inverse modeling: A model study, Global Biogeochem. Cycles, 14(1), 407–428, 2000.

Grell, G. A., Dudhia, J., and Stauffer, D. R.: A Description of the Fifth-Generation Penn State/NCAR Mesoscale Model (MM5). NCAR/TN-398+STR, NCAR Technical Note, Mesoscale and Microscale Meteorology Division, National Center for Atmospheric Research, Boulder, Colorado, pp. 122, June 1995.

Gurney, K. R., Law, R. M., Denning, A. S., Rayner, P. J., Baker, D., Bousquet, P., Bruhwiler, L., Chen, Y.-H., Ciais, P., Fan, S., Fung, I. Y., Gloor, M., Heimann, M., Higuchi, K., John, J., Maki, T., Maksyutov, S., Masari, K., Peylin, P., Prather, M., Pak, B. C., Randerson, J., Sarmiento, J., Taguchi, S., Takahashi T., and Yuen, C.-W.: Towards robust regional estimates of CO_2 sources and sinks using atmospheric transport models, Nature, 415, 626–630, 2002.

Gurney, K. R., Law, R. M., Denning, A. S., Rayner, P. J., Baker, D., Bousquet, P., Bruhwiler, L., Chen, Y.-H., Ciais, P., Fan, S., Fung, I. Y., Gloor, M., Heimann, M., Higuchi, K., John, J., Kowalczyk, E., Maki, T., Maksyutov, S., Peylin, P., Prather, M., Pak, B. C., Sarmiento, J., Taguchi, S., Takahashi T., and Yuen, C.-W.: TransCom 3 CO_2 inversion intercomparison: 1. Annual mean control results and sensitivity to transport and prior flux information, Tellus, 55B, 555–579, 2003.

Hansen, K. M., Christensen, J. H., Brandt, J., Frohn, L. M.,

and Geels, C.: Modelling atmospheric transport of alpha-hexachlorocyclohexane in the Northern Hemisphere with a 3-D dynamical model: DEHM-POP, Atmos. Chem. Phys., 4, 1125–1137, 2004, http://www.atmos-chem-phys.net/4/1125/2004/.

Haszpra, L.: On the representativeness of carbon dioxide measurements, J. Geophys. Res., 104(D21), 26 953–26 960, 1999.

Hauglustaine, D. A., Hourdin, F., Jourdain, L., Filiberti, M., Walters, S., Lamarque, J., and Holland, E. A.: Interactive chemistry in the Laboratoire de Metorologie Dynamique general circulation model: Description and background tropospheric chemistry evaluation, J. Geophys. Res., 109, D04314, doi:10.1029/2003JD003,957, 2004.

Hess, P. G., Flocke, S., Lamarque, J.-F., Barth, M. C., and Madronich, S.: Episodic modeling of the chemical structure of the troposphere as revealed during the spring MLOPEX intensive, J. Geophys. Res., 105(D22), 26 809–26 839, 2000.

Heimann, M.: The global atmsopheric transport model TM2, Tech. Rep. 10, Max-Planck-Inst. für Meteorologie, Hamburg, Germany, 1996.

Kjellström, E., Holmèn, K., Eneroth, K., and Engardt, M.: Summertime Siberian CO_2 simulations with the regional transport model MATCH: a feasibility study of carbon uptake calculations from EUROSIB data, Tellus, 54B, 834–849, 2002.

Kowalski, S., Sartore, M., Burlett, R., Berbigier, P., and Loustau, D.: The annual carbon budget of a French pine forest (Pinus pinaster) following harvest, Global Change Biol., 9, 1051–1065, 2003.

Lafont, S., Kergoat, L., Dedieu, G., Chevillard, A., Karstens, U., and Kolle, O.: Spatial and temporal variability of land CO_2 fluxes estimated with remote sensing and analysis data over western Eurasia, Tellus, 54B, 820–833, 2002.

Langmann, B.: Numerical modelling of regional scale transport and photochemistry directly together with meteorological processes, Atmos. Environ., 34, 3585–3598, 2000.

Levin, I., Graul, R., and Trivett, N. B. A.: Long-term observations of atmospheric CO_2 and carbon isotopes at continental sites in Germany, Tellus, 47B, 23–34, 1995.

Levin, I., Kromer, B., Schmidt, M., and Sartorius, H.: A novel approach for independent budgeting of fossil fuel CO_2 over Europe by $^{14}CO_2$ observations, Geophys. Res. Lett., 30, 23, 2194, doi:10.1029/2003GLO18477, 2003.

Law, R. M., Rayner, P. J., Denning, A. S., Erickson, D., Fung, I. Y., Heimann, M., Piper, S. C., Ramonet, M., Taguchi, S., Taylor, J. A., Trudinger, C. M., and Watterson, I. G.: Variations in modeled atmospheric transport of carbon dioxide and the consequences for CO_2 inversions, Global Biogeochem. Cy., 10, 783–796, 1996.

Law, R. M., Rayner, P. J., Steele, L. P., and Enting, I. G.: Using high temporal frequency data for CO_2 inversions, Global Biogeochem. Cy., 16(4), 1053, doi:10.1029/2001GB001593, 2002.

Law, R. M., Peters, W., Rodenbeck, C., Bruhwiler, L., and TC modellers: An intercomparison of the diurnal and synoptic behaviour of global transport models, in: 7th International Carbon Dioxide Conference: abstracts, Broomfield, Colo. Boulder, Colo., Committee of the Seventh International Carbon Dioxide Conference, 2 p., 2005.

Majewski, D.: The Europamodell of the Deutscher Wetterdienst, ECMWF course, Numerical methods in atmospheric models, Vol. 2., pp. 147–191, 1991.

Marland, G., Boden, T. A., and Andres, R. J.: Global, Regional, and National CO_2 emissions, in: Trends, A compendium of data on global change, Carbon Dioxide Information Analysis Center, Oak Ridge National Laboratory, U.S. Department of Energy, Oak Ridge, Tenn., USA, 2003.

Olivier, J. G. J., Bouwman, A. F., van der Maas, C. W. M., Berdowski, J. M., Veldt, C., Bloos, J. P. J., Visschedijk, A. J. H., Zandveld P. J., and Haverlag, J. L.: Description of EDGAR Version 2.0: A set of global emission inventories of greenhouse gases and ozone-depleting substances for all anthropogenic and most natural sources on a per country basis and on $1^\circ \times 1^\circ$ grid, National Institute of Public Health and the Environment (RVIM) report nr. 771060 002/TNO-MEP report nr. R96/119, 1996.

Peylin, P., Rayner, P. J., Bousquet, P., Carouge, C., Hourdin, F., Heinrich, P., Ciais, P., and AEROCARB contributors: Daily CO_2 flux estimates over Europe from continuous atmospheric measurements: 1. Inverse methodology, Atmos. Chem. Phys., 5, 3173–3186, 2005, http://www.atmos-chem-phys.net/5/3173/2005/.

Rayner, P. J. and Law, R. M.: A comparison of modelled responses to prescribed CO_2 sources, Tech. Pap. 36, 82 pp., Div. of Atmos. Res., Commonw. Sci. Ind. Res. Organ., Aspendale, Victoria, Australia, 1995.

Rayner, P. J., Enting, I. G., Francey R. J., and Langenfelds, R.: Reconstructing the recent carbon cycle from atmospheric CO_2, $d^{13}C$ and O2/N2 observations, Tellus, 51B, 2, 213–232, 1999.

Ruimy, A., Dedieu G., and Saugier, B.: TURC: A diagnostic model of continental gross primary productivity and net primary productivity, Global Biogeochem. Cy., 10, 2, 269–285, 1996.

Rödenbeck, C., Houweling, S., Gloor, M., and Heimann, M.: CO_2 flux history 1982–2001 inferred from atmospheric data using a global inversion of atmospheric transport, Atmos. Chem. Phys., 3 1919–1964, 2003.

Schmidt, M., Graul, R., Sartorius, H., and Levin, I.: The Schauinsland CO_2 record: 30 years of continental observations and their implications for the variability of the European CO_2 budget, J. Geophys. Res., 108(D19), 4619, doi:10.1029/2002JD003085, 2003.

Takahashi, T., Wanninkhof, R. H., Feely, R. A., Weiss, R. F., Chipman, D. W., Bates, N., Olafsson, J., Sabine C., and Sutherland, S. C.: Net sea-air CO_2 flux over the global oceans: an improved estimate based on the sea-air CO_2 difference, in: Proceedings of the 2nd International Symposium, CO_2 in the Oceans, Center for Global Environmental Research, National Institute for Environmental Studies, Tsukuba, edited by: Nojiri, Y., 9–14, 1999.

Taylor, K. E.: Summarizing multiple aspects of model performance in a single diagram, J. Geophys. Res., 106(D7), 7183–7192, 2001.

Wanninkhof, R.: Relationships between wind speed and gas exchange over the ocean, J. Geophys. Res., 97, 5, 7373–7382, 1992.